PHYSICAL REVIEW C **83**, 024909 (2011)

# Nuclear modification factors of $\phi$ mesons in $d$ + Au, Cu + Cu, and Au + Au collisions at $\sqrt{s_{NN}} = 200$ GeV

A. Adare,[11] S. Afanasiev,[26] C. Aidala,[12,40] N. N. Ajitanand,[57] Y. Akiba,[51,52] H. Al-Bataineh,[46] J. Alexander,[57] A. Al-Jamel,[46] A. Angerami,[12] K. Aoki,[33,51] N. Apadula,[58] L. Aphecetche,[59] Y. Aramaki,[10] R. Armendariz,[46] S. H. Aronson,[5] J. Asai,[52] E. T. Atomssa,[34] R. Averbeck,[58] T. C. Awes,[47] B. Azmoun,[5] V. Babintsev,[22] M. Bai,[4] G. Baksay,[18] L. Baksay,[18] A. Baldisseri,[14] K. N. Barish,[6] P. D. Barnes,[36] B. Bassalleck,[45] A. T. Basye,[1] S. Bathe,[6] S. Batsouli,[12,47] V. Baublis,[50] F. Bauer,[6] C. Baumann,[41] A. Bazilevsky,[5] S. Belikov,[5,25,*] R. Belmont,[63] R. Bennett,[58] A. Berdnikov,[54] Y. Berdnikov,[54] J. H. Bhom,[66] A. A. Bickley,[11] M. T. Bjorndal,[12] D. S. Blau,[32] J. G. Boissevain,[36] J. S. Bok,[66] H. Borel,[14] N. Borggren,[57] K. Boyle,[58] M. L. Brooks,[36] D. S. Brown,[46] D. Bucher,[41] H. Buesching,[5] V. Bumazhnov,[22] G. Bunce,[5,52] J. M. Burward-Hoy,[36] S. Butsyk,[36,58] S. Campbell,[58] A. Caringi,[42] J.-S. Chai,[28] B. S. Chang,[66] J. L. Charvet,[14] C. H. Chen,[58] S. Chernichenko,[22] J. Chiba,[29] C. Y. Chi,[12] M. Chiu,[5,12,23] I. J. Choi,[66] J. B. Choi,[8] R. K. Choudhury,[3] P. Christiansen,[38] T. Chujo,[62,63] P. Chung,[57] A. Churyn,[22] O. Chvala,[6] V. Cianciolo,[47] Z. Citron,[58] C. R. Cleven,[20] Y. Cobigo,[14] B. A. Cole,[12] M. P. Comets,[48] Z. Conesa del Valle,[34] M. Connors,[58] P. Constantin,[25,36] M. Csanád,[16] T. Csörgő,[30] T. Dahms,[58] S. Dairaku,[33,51] I. Danchev,[63] K. Das,[19] A. Datta,[40] G. David,[5] M. K. Dayananda,[20] M. B. Deaton,[1] K. Dehmelt,[18] H. Delagrange,[59] A. Denisov,[22] D. d'Enterria,[12] A. Deshpande,[52,58] E. J. Desmond,[5] K. V. Dharmawardane,[46] O. Dietzsch,[55] A. Dion,[25,58] M. Donadelli,[55] L. D'Orazio,[39] J. L. Drachenberg,[1] O. Drapier,[34] A. Drees,[58] K. A. Drees,[4] A. K. Dubey,[65] J. M. Durham,[58] A. Durum,[22] D. Dutta,[3] V. Dzhordzhadze,[6,60] S. Edwards,[19] Y. V. Efremenko,[47] J. Egdemir,[58] F. Ellinghaus,[11] W. S. Emam,[6] T. Engelmore,[12] A. Enokizono,[21,35,47] H. En'yo,[51,52] B. Espagnon,[48] S. Esumi,[62] K. O. Eyser,[6] B. Fadem,[42] D. E. Fields,[45,52] M. Finger Jr.,[7,26] M. Finger,[7,26] F. Fleuret,[34] S. L. Fokin,[32] B. Forestier,[37] Z. Fraenkel,[65,*] J. E. Frantz,[12,58] A. Franz,[5] A. D. Frawley,[19] K. Fujiwara,[51] Y. Fukao,[33,51] S. Y. Fung,[6] T. Fusayasu,[44] S. Gadrat,[37] I. Garishvili,[60] F. Gastineau,[59] M. Germain,[59] A. Glenn,[11,35,60] H. Gong,[58] M. Gonin,[34] J. Gosset,[14] Y. Goto,[51,52] R. Granier de Cassagnac,[34] N. Grau,[12,25] S. V. Greene,[63] G. Grim,[36] M. Grosse Perdekamp,[23,52] T. Gunji,[10] H.-Å. Gustafsson,[38,*] T. Hachiya,[21,51] A. Hadj Henni,[59] C. Haegemann,[45] J. S. Haggerty,[5] M. N. Hagiwara,[1] K. I. Hahn,[17] H. Hamagaki,[10] J. Hamblen,[60] J. Hanks,[12] R. Han,[49] H. Harada,[21] E. P. Hartouni,[35] K. Haruna,[21] M. Harvey,[5] E. Haslum,[38] K. Hasuko,[51] R. Hayano,[10] M. Heffner,[35] T. K. Hemmick,[58] T. Hester,[6] J. M. Heuser,[51] X. He,[20] H. Hiejima,[23] J. C. Hill,[25] R. Hobbs,[45] M. Hohlmann,[18] M. Holmes,[63] W. Holzmann,[12,57] K. Homma,[21] B. Hong,[31] T. Horaguchi,[21,51,61] D. Hornback,[60] S. Huang,[63] M. G. Hur,[28] T. Ichihara,[51,52] R. Ichimiya,[51] H. Iinuma,[33,51] Y. Ikeda,[62] K. Imai,[33,51] M. Inaba,[62] Y. Inoue,[53,51] D. Isenhower,[1] L. Isenhower,[1] M. Ishihara,[51] T. Isobe,[10] M. Issah,[57,63] A. Isupov,[26] D. Ivanischev,[50] Y. Iwanaga,[21] B. V. Jacak,[58,†] J. Jia,[5,12,57] X. Jiang,[36] J. Jin,[12] O. Jinnouchi,[52] B. M. Johnson,[5] T. Jones,[1] K. S. Joo,[43] D. Jouan,[48] D. S. Jumper,[1] F. Kajihara,[10,51] S. Kametani,[10,64] N. Kamihara,[51,61] J. Kamin,[58] M. Kaneta,[52] J. H. Kang,[66] H. Kanou,[51,61] J. Kapustinsky,[36] K. Karatsu,[33] M. Kasai,[53,51] T. Kawagishi,[62] D. Kawall,[40,52] M. Kawashima,[53,51] A. V. Kazantsev,[32] S. Kelly,[11] T. Kempel,[25] A. Khanzadeev,[50] K. M. Kijima,[21] J. Kikuchi,[64] A. Kim,[17] B. I. Kim,[31] D. H. Kim,[43] D. J. Kim,[27,66] E. J. Kim,[8] E. Kim,[56] Y.-J. Kim,[23] Y.-S. Kim,[28] E. Kinney,[11] Á. Kiss,[16] E. Kistenev,[5] A. Kiyomichi,[51] J. Klay,[35] C. Klein-Boesing,[41] L. Kochenda,[50] V. Kochetkov,[22] B. Komkov,[50] M. Konno,[62] J. Koster,[23] D. Kotchetkov,[6] D. Kotov,[54] A. Kozlov,[65] A. Král,[13] A. Kravitz,[12] P. J. Kroon,[5] J. Kubart,[7,24] G. J. Kunde,[36] N. Kurihara,[10] K. Kurita,[53,51] M. Kurosawa,[51] M. J. Kweon,[31] Y. Kwon,[60,66] G. S. Kyle,[46] R. Lacey,[57] Y. S. Lai,[12] J. G. Lajoie,[25] A. Lebedev,[25] Y. Le Bornec,[48] S. Leckey,[58] D. M. Lee,[36] J. Lee,[17] K. B. Lee,[31] K. S. Lee,[31] M. K. Lee,[66] T. Lee,[56] M. J. Leitch,[36] M. A. L. Leite,[55] B. Lenzi,[55] P. Lichtenwalner,[42] P. Liebing,[52] H. Lim,[56] L. A. Linden Levy,[11] T. Liška,[13] A. Litvinenko,[26] H. Liu,[36] M. X. Liu,[36] X. Li,[9] X. H. Li,[6] B. Love,[63] D. Lynch,[5] C. F. Maguire,[63] Y. I. Makdisi,[4,5] A. Malakhov,[26] M. D. Malik,[45] V. I. Manko,[32] E. Mannel,[12] Y. Mao,[49,51] L. Mašek,[7,24] H. Masui,[62] F. Matathias,[12,58] M. C. McCain,[23] M. McCumber,[58] P. L. McGaughey,[36] N. Means,[58] B. Meredith,[23] Y. Miake,[62] T. Mibe,[29] A. C. Mignerey,[39] P. Mikeš,[7,24] K. Miki,[62] T. E. Miller,[63] A. Milov,[5,58] S. Mioduszewski,[5] G. C. Mishra,[20] M. Mishra,[2] J. T. Mitchell,[5] M. Mitrovski,[57] A. K. Mohanty,[3] H. J. Moon,[43] Y. Morino,[10] A. Morreale,[6] D. P. Morrison,[5] J. M. Moss,[36] T. V. Moukhanova,[32] D. Mukhopadhyay,[63] T. Murakami,[33] J. Murata,[53,51] S. Nagamiya,[29] Y. Nagata,[62] J. L. Nagle,[11] M. Naglis,[65] M. I. Nagy,[30] I. Nakagawa,[51,52] Y. Nakamiya,[21] K. R. Nakamura,[33] T. Nakamura,[21,51] K. Nakano,[51,61] S. Nam,[17] J. Newby,[35] M. Nguyen,[58] M. Nihashi,[21] B. E. Norman,[36] R. Nouicer,[5] A. S. Nyanin,[32] J. Nystrand,[38] C. Oakley,[20] E. O'Brien,[5] S. X. Oda,[10] C. A. Ogilvie,[25] H. Ohnishi,[51] I. D. Ojha,[63] K. Okada,[52] M. Oka,[62] O. O. Omiwade,[1] Y. Onuki,[51] A. Oskarsson,[38] I. Otterlund,[38] M. Ouchida,[21] K. Ozawa,[10] R. Pak,[5] D. Pal,[63] A. P. T. Palounek,[36] V. Pantuev,[58] V. Papavassiliou,[46] I. H. Park,[17] J. Park,[56] S. K. Park,[31] W. J. Park,[31] S. F. Pate,[46] H. Pei,[25] J.-C. Peng,[23] H. Pereira,[14] V. Peresedov,[26] D. Yu. Peressounko,[32] R. Petti,[58] C. Pinkenburg,[5] R. P. Pisani,[5] M. Proissl,[58] M. L. Purschke,[5] A. K. Purwar,[36,58] H. Qu,[20] J. Rak,[25,27,45] A. Rakotozafindrabe,[34] I. Ravinovich,[65] K. F. Read,[47,60] S. Rembeczki,[18] M. Reuter,[58] K. Reygers,[41] V. Riabov,[50] Y. Riabov,[50] E. Richardson,[39] D. Roach,[63] G. Roche,[37] S. D. Rolnick,[6] A. Romana,[34,*] M. Rosati,[25] C. A. Rosen,[11] S. S. E. Rosendahl,[38] P. Rosnet,[37] P. Rukoyatkin,[26] P. Ružička,[24] V. L. Rykov,[51] S. S. Ryu,[66] B. Sahlmueller,[41] N. Saito,[29,33,51] T. Sakaguchi,[5,10,64] S. Sakai,[62] K. Sakashita,[51,61] H. Sakata,[21] V. Samsonov,[50] S. Sano,[10,64] H. D. Sato,[33,51] S. Sato,[5,29,62] T. Sato,[62] S. Sawada,[29] K. Sedgwick,[6] J. Seele,[11] R. Seidl,[23] V. Semenov,[22] R. Seto,[6] D. Sharma,[65] T. K. Shea,[5] I. Shein,[22] A. Shevel,[50,57] T.-A. Shibata,[51,61] K. Shigaki,[21] M. Shimomura,[62] T. Shohjoh,[62] K. Shoji,[33,51] P. Shukla,[3] A. Sickles,[5,58] C. L. Silva,[25,55] D. Silvermyr,[47] C. Silvestre,[14] K. S. Sim,[31] B. K. Singh,[2] C. P. Singh,[2] V. Singh,[2] S. Skutnik,[25] M. Slunečka,[7,26] W. C. Smith,[1] A. Soldatov,[22] R. A. Soltz,[35] W. E. Sondheim,[36] S. P. Sorensen,[60] I. V. Sourikova,[5] F. Staley,[14] P. W. Stankus,[47] E. Stenlund,[38] M. Stepanov,[46] A. Ster,[30]

 

S. P. Stoll,[5] T. Sugitate,[21] C. Suire,[48] A. Sukhanov,[5] J. P. Sullivan,[36] J. Sziklai,[30] T. Tabaru,[52] S. Takagi,[62] E. M. Takagui,[55] A. Taketani,[51,52] R. Tanabe,[62] K. H. Tanaka,[29] Y. Tanaka,[44] S. Taneja,[58] K. Tanida,[33,51,52] M. J. Tannenbaum,[5] S. Tarafdar,[2] A. Taranenko,[57] P. Tarján,[15] H. Themann,[58] D. Thomas,[1] T. L. Thomas,[45] M. Togawa,[33,51,52] A. Toia,[58] J. Tojo,[51] L. Tomášek,[24] H. Torii,[21,51] R. S. Towell,[1] V.-N. Tram,[34] I. Tserruya,[65] Y. Tsuchimoto,[21,51] S. K. Tuli,[2] H. Tydesjö,[38] N. Tyurin,[22] C. Vale,[5,25] H. Valle,[63] H. W. van Hecke,[36] E. Vazquez-Zambrano,[12] A. Veicht,[23] J. Velkovska,[63] R. Vértesi,[15,30] A. A. Vinogradov,[32] M. Virius,[13] V. Vrba,[24] E. Vznuzdaev,[50] M. Wagner,[33,51] D. Walker,[58] X. R. Wang,[46] D. Watanabe,[21] K. Watanabe,[62] Y. Watanabe,[51,52] F. Wei,[25] J. Wessels,[41] S. N. White,[5] N. Willis,[48] D. Winter,[12] C. L. Woody,[5] R. M. Wright,[1] M. Wysocki,[11] W. Xie,[6,52] Y. L. Yamaguchi,[10,64] K. Yamaura,[21] R. Yang,[23] A. Yanovich,[22] Z. Yasin,[6] J. Ying,[20] S. Yokkaichi,[51,52] G. R. Young,[47] I. Younus,[45] Z. You,[49] I. E. Yushmanov,[32] W. A. Zajc,[12] O. Zaudtke,[41] C. Zhang,[12,47] S. Zhou,[9] J. Zimányi,[30,*] and L. Zolin[26]

(PHENIX Collaboration)

[1]*Abilene Christian University, Abilene, Texas 79699, USA*
[2]*Department of Physics, Banaras Hindu University, Varanasi 221005, India*
[3]*Bhabha Atomic Research Centre, Bombay 400 085, India*
[4]*Collider-Accelerator Department, Brookhaven National Laboratory, Upton, New York 11973-5000, USA*
[5]*Physics Department, Brookhaven National Laboratory, Upton, New York 11973-5000, USA*
[6]*University of California-Riverside, Riverside, California 92521, USA*
[7]*Charles University, Ovocný trh 5, Praha 1, CZ-116 36, Prague, Czech Republic*
[8]*Chonbuk National University, Jeonju 561-756, Korea*
[9]*China Institute of Atomic Energy (CIAE), Beijing, People's Republic of China*
[10]*Center for Nuclear Study, Graduate School of Science, University of Tokyo, 7-3-1 Hongo, Bunkyo, Tokyo 113-0033, Japan*
[11]*University of Colorado, Boulder, Colorado 80309, USA*
[12]*Columbia University, New York, New York 10027, USA and Nevis Laboratories, Irvington, New York 10533, USA*
[13]*Czech Technical University, Zikova 4, CZ-166 36 Prague 6, Czech Republic*
[14]*Dapnia, CEA Saclay, F-91191 Gif-sur-Yvette, France*
[15]*Debrecen University, H-4010 Debrecen, Egyetem tér 1, Hungary*
[16]*ELTE, Eötvös Loránd University, H-1117 Budapest, Pázmány Péter sétány 1/A, Hungary*
[17]*Ewha Womans University, Seoul 120-750, Korea*
[18]*Florida Institute of Technology, Melbourne, Florida 32901, USA*
[19]*Florida State University, Tallahassee, Florida 32306, USA*
[20]*Georgia State University, Atlanta, Georgia 30303, USA*
[21]*Hiroshima University, Kagamiyama, Higashi-Hiroshima 739-8526, Japan*
[22]*IHEP Protvino, State Research Center of Russian Federation, Institute for High Energy Physics, Protvino RU-142281, Russia*
[23]*University of Illinois at Urbana-Champaign, Urbana, Illinois 61801, USA*
[24]*Institute of Physics, Academy of Sciences of the Czech Republic, Na Slovance 2, CZ-182 21 Prague 8, Czech Republic*
[25]*Iowa State University, Ames, Iowa 50011, USA*
[26]*Joint Institute for Nuclear Research, RU-141980 Dubna, Moscow Region, Russia*
[27]*Helsinki Institute of Physics, University of Jyväskylä, P. O. Box 35, FI-40014 Jyväskylä, Finland*
[28]*KAERI, Cyclotron Application Laboratory, Seoul, Korea*
[29]*KEK, High Energy Accelerator Research Organization, Tsukuba, Ibaraki 305-0801, Japan*
[30]*KFKI Research Institute for Particle and Nuclear Physics of the Hungarian Academy of Sciences (MTA KFKI RMKI), P. O. Box 49, H-1525 Budapest 114, Budapest, Hungary*
[31]*Korea University, Seoul 136-701, Korea*
[32]*Russian Research Center "Kurchatov Institute," Moscow 123098, Russia*
[33]*Kyoto University, Kyoto 606-8502, Japan*
[34]*Laboratoire Leprince-Ringuet, Ecole Polytechnique, CNRS-IN2P3, Route de Saclay, F-91128 Palaiseau, France*
[35]*Lawrence Livermore National Laboratory, Livermore, California 94550, USA*
[36]*Los Alamos National Laboratory, Los Alamos, New Mexico 87545, USA*
[37]*LPC, Université Blaise Pascal, CNRS-IN2P3, Clermont-Fd, F-63177 Aubiere Cedex, France*
[38]*Department of Physics, Lund University, Box 118, SE-221 00 Lund, Sweden*
[39]*University of Maryland, College Park, Maryland 20742, USA*
[40]*Department of Physics, University of Massachusetts, Amherst, Massachusetts 01003-9337, USA*
[41]*Institut fur Kernphysik, University of Muenster, D-48149 Muenster, Germany*
[42]*Muhlenberg College, Allentown, Pennsylvania 18104-5586, USA*
[43]*Myongji University, Yongin, Kyonggido 449-728, Korea*
[44]*Nagasaki Institute of Applied Science, Nagasaki-shi, Nagasaki 851-0193, Japan*
[45]*University of New Mexico, Albuquerque, New Mexico 87131, USA*
[46]*New Mexico State University, Las Cruces, New Mexico 88003, USA*

[47]*Oak Ridge National Laboratory, Oak Ridge, Tennessee 37831, USA*
[48]*IPN-Orsay, Universite Paris Sud, CNRS-IN2P3, Boîte Postale 1, F-91406 Orsay, France*
[49]*Peking University, Beijing, People's Republic of China*
[50]*PNPI, Petersburg Nuclear Physics Institute, Gatchina, Leningrad region RU-188300, Russia*
[51]*RIKEN Nishina Center for Accelerator-Based Science, Wako, Saitama 351-0198, Japan*
[52]*RIKEN BNL Research Center, Brookhaven National Laboratory, Upton, New York 11973-5000, USA*
[53]*Department of Physics, Rikkyo University, 3-34-1 Nishi-Ikebukuro, Toshima, Tokyo 171-8501, Japan*
[54]*Saint Petersburg State Polytechnic University, St. Petersburg 195251, Russia*
[55]*Universidade de São Paulo, Instituto de Física, Caixa Postal 66318, São Paulo CEP05315-970, Brazil*
[56]*System Electronics Laboratory, Seoul National University, Seoul, Korea*
[57]*Department of Chemistry, Stony Brook University, Stony Brook, SUNY, New York 11794-3400, USA*
[58]*Department of Physics and Astronomy, Stony Brook University, SUNY, Stony Brook, New York 11794, USA*
[59]*SUBATECH (Ecole des Mines de Nantes, CNRS-IN2P3, Université de Nantes) Boîte Postale, F-20722-44307 Nantes, France*
[60]*University of Tennessee, Knoxville, Tennessee 37996, USA*
[61]*Department of Physics, Tokyo Institute of Technology, Oh-okayama, Meguro, Tokyo 152-8551, Japan*
[62]*Institute of Physics, University of Tsukuba, Tsukuba, Ibaraki 305, Japan*
[63]*Vanderbilt University, Nashville, Tennessee 37235, USA*
[64]*Advanced Research Institute for Science and Engineering, Waseda University, 17 Kikui-cho, Shinjuku-ku, Tokyo 162-0044, Japan*
[65]*Weizmann Institute, Rehovot 76100, Israel*
[66]*Yonsei University, IPAP, Seoul 120-749, Korea*
(Received 20 April 2010; published 18 February 2011)

The PHENIX experiment at the Relativistic Heavy Ion Collider has performed systematic measurements of $\phi$ meson production in the $K^+K^-$ decay channel at midrapidity in $p + p$, $d$ + Au, Cu + Cu, and Au + Au collisions at $\sqrt{s_{NN}} = 200$ GeV. Results are presented on the $\phi$ invariant yield and the nuclear modification factor $R_{\rm AA}$ for Au + Au and Cu + Cu, and $R_{\rm dA}$ for $d$ + Au collisions, studied as a function of transverse momentum ($1 < p_T < 7$ GeV/$c$) and centrality. In central and midcentral Au + Au collisions, the $R_{\rm AA}$ of $\phi$ exhibits a suppression relative to expectations from binary scaled $p + p$ results. The amount of suppression is smaller than that of the $\pi^0$ and the $\eta$ in the intermediate $p_T$ range (2–5 GeV/$c$), whereas, at higher $p_T$, the $\phi$, $\pi^0$, and $\eta$ show similar suppression. The baryon (proton and antiproton) excess observed in central Au + Au collisions at intermediate $p_T$ is not observed for the $\phi$ meson despite the similar masses of the proton and the $\phi$. This suggests that the excess is linked to the number of valence quarks in the hadron rather than its mass. The difference gradually disappears with decreasing centrality, and, for peripheral collisions, the $R_{\rm AA}$ values for both particle species are consistent with binary scaling. Cu + Cu collisions show the same yield and suppression as Au + Au collisions for the same number of $N_{\rm part}$. The $R_{\rm dA}$ of $\phi$ shows no evidence for cold nuclear effects within uncertainties.

DOI: 10.1103/PhysRevC.83.024909 PACS number(s): 21.65.Jk, 25.75.Dw

## I. INTRODUCTION

Measurements of hadron spectra from $p + p$ and nucleus-nucleus collisions at the Relativistic Heavy Ion Collider (RHIC) provide a means to study the mechanisms of particle production and the properties of the medium formed in relativistic heavy ion collisions. At low transverse momentum $p_T < 2$ GeV/$c$, where the bulk of particles are produced, hadron production is governed by soft processes characterized by low-momentum transfer. The particle yields and the evolution of the interacting system are successfully described within the framework of thermal and hydrodynamical models [1–5].

At high transverse momentum $p_T > 5$ GeV/$c$, hard scattering processes become the dominant contribution. Because of the large momentum transfer involved, the parton-parton scattering cross sections are amenable to perturbative QCD (pQCD) description, and hadron production can be calculated by using initial-state parton distribution functions and final-state fragmentation functions. Modifications to the hadron yields are expected in nucleus-nucleus collisions because of the interaction of the scattered parton with the hot and dense medium formed [6–8]. In the absence of interaction with the medium, the hard scatterings and the resulting hadron yields should scale with the number of binary nucleon-nucleon collisions ($N_{\rm coll}$), whereas, in the medium, the yields are suppressed (jet quenching [9]) because of parton energy loss through gluon bremsstrahlung. High-$p_T$ hadron suppression consistent with this scenario has been discovered in Au + Au collisions at RHIC [10–12]. The same suppression by a factor of ∼5 is observed for $\pi^0$ and $\eta$ production, whereas, direct photons that do not interact with the medium, follow the expected binary scaling [13]. Single electrons that originate from the semileptonic decays of mesons that contain heavy quarks

*Deceased.
†PHENIX spokesperson: jacak@skipper.physics.sunysb.edu

(charm and bottom) exhibit a large suppression at high $p_T$, similar within the experimental uncertainties to that of $\pi^0$ and $\eta$, which present a challenge for the bremsstrahlung explanation [14].

At intermediate transverse momentum $2 < p_T$ (GeV/$c$) $<$ 5, suppression of binary scaled production is observed for light $\pi^0$ and $\eta$ mesons but not for protons and antiprotons in mid-central and central Au + Au collisions [15]. The $p/\pi$ and $\bar{p}/\pi$ ratios increase with centrality and exceed the values measured in $p + p$ by a factor of 3–5 in the most central collisions. A different suppression pattern between baryons and mesons is also observed for strange hadrons $\Lambda$ and $K_S^0$ [16,17]. These baryon-meson differences in suppression are inconsistent with the picture of hadron production through hard scattering followed by partonic energy loss in medium and hadronization in vacuum according to the universal fragmentation functions. This poses the question whether hard scattering is the dominant source of baryon production at intermediate $p_T$. Studies of jet-like dihadron correlations in Au + Au collisions [18,19] imply nearly equal importance of the jet fragmentation as a production mechanism for mesons and baryons, except for the most central collisions. Therefore, the interpretation of the baryon nonsuppression results requires another particle production mechanism in addition to jet fragmentation at intermediate $p_T$.

There have been attempts to describe the different behavior of baryons and mesons through the strong radial flow that boosts particles with larger mass to higher $p_T$ [20,21], through the recombination of soft and hard massive partons [22–24], through the interplay of the jet-quenched hard component and phenomenological soft-to-moderate $p_T$ baryon junction component [25], or through the QCD color transparency of higher-twist contributions to inclusive hadroproduction cross sections, where baryons are produced directly in a short-distance subprocess [26]. Although several models reproduce $p_T$ spectra, particle ratios, and elliptic flow for different hadrons reasonably well, the relative contributions from the different processes are difficult to infer.

The $\phi$ meson is a very rich probe of the medium formed in heavy ion collisions because it is sensitive to several aspects of the collision, which include strangeness enhancement and chiral-symmetry restoration as well as energy loss and the nuclear modification factor [27–31], which is the focus of this paper. Due to its small inelastic cross section for interaction with nonstrange hadrons [27,32], the $\phi$ meson is less affected by late hadronic rescattering and better reflects the initial evolution of the system. By being a meson with a mass comparable to that of the proton, it is interesting to see how the $\phi$ meson fits within the meson-baryon pattern described previously; by being a pure $s\bar{s}$ state, it puts additional constraints on the energy-loss and recombination models.

This paper presents systematic PHENIX measurements of $\phi$ meson production via the $K^+K^-$ decay channel at $\sqrt{s_{NN}} = 200$ GeV, which includes the first PHENIX results in $p + p$, $d$ + Au, and Cu + Cu collisions and new results in Au + Au collisions. The latter have much higher statistics and a finer centrality binning in comparison to the previously published PHENIX results [28]. The results benefit from three different techniques, which involve different levels of kaon identification in the analyses. These, combined with the high statistics of the analyzed data samples, allow for the extension of the $p_T$ range of the measurements up to $p_T = 7.0$ GeV/$c$ in all collision systems. The higher $p_T$ reach and the higher precision of the data allow for sharper conclusions with respect to earlier results [28,30]. The Cu + Cu measurements are complementary to those on Au + Au and allow the study of nuclear effects with different nuclear overlap geometry for the same $N_{\rm part}$ and with smaller $N_{\rm part}$ uncertainties for $N_{\rm part} < 100$.

The measurement of the $\phi$ meson production in $d$ + Au collisions is important for understanding cold nuclear matter effects that are of interest by themselves and are also essential for the interpretation of heavy ion collisions. As shown in Ref. [33], in the intermediate $p_T$ range, charged pions practically are not enhanced in comparison to the binary scaled $p + p$ yield, whereas, protons and antiprotons exhibit some enhancement of $\sim$30% in the most central collisions. The mechanism of multiple soft rescattering of partons in the initial state, which is usually invoked as the origin of the Cronin effect, does not explain this meson-baryon difference. One possible explanation comes from recombination models [34] in which baryons gain higher transverse momentum from recombination of three quarks in the final state in comparison to mesons consisting of only two quarks. Measurement of the Cronin effect for the $\phi$ mesons can provide additional constraints for the models that try to explain these cold nuclear effects.

## II. EXPERIMENTAL SETUP AND DATA ANALYSIS

We report on the measurements of $\phi$ mesons at midrapidity in the $K^+K^-$ decay channel in $p + p$, $d$ + Au, Cu + Cu, and Au + Au collisions at $\sqrt{s_{NN}} = 200$ GeV by using data collected by the PHENIX experiment during the 2004, 2005, and 2008 physics runs. A detailed description of the PHENIX detector can be found elsewhere [35]. The measurements were performed by using the two PHENIX central arms, each covering 90° in azimuth at midrapidity ($|\eta| < 0.35$). The tracking of charged particles and the measurement of their momentum with typical resolution of $\delta p/p = 0.7 \oplus 1.1\% p$ [GeV/$c$] are performed by using the drift chambers and the first layer of the pad chambers (PCs). To reduce the background at high $p_T$, tracks are required to have a matching confirmation in the third layer of the PC or the electromagnetic calorimeter. Kaons are identified by using the time-of-flight (TOF) detector, which covers approximately 1/3 of the acceptance in one of the central arms. With a time resolution of $\sim$115 ps, the TOF allows for clear $\pi/K$ separation in the range of transverse momentum from 0.3 GeV/$c$ to 2.2 GeV/$c$ by using a $2\sigma$ $p_T$-dependent mass-squared selection cut as described in Ref. [28].

The beam-beam counters (BBCs) and zero-degree calorimeters (ZDCs) are dedicated subsystems that determine the collision vertex along the beam axis ($z_{\rm vtx}$) and the event centrality and also provide the minimum bias interaction trigger. Events are categorized into centrality classes by using two-dimensional cuts in the space of BBC charge versus ZDC energy [36] for Au + Au collisions or only by the amount of charge deposited in the BBC [12,37] for $d$ + Au and Cu + Cu collisions.

In any particular event, one cannot distinguish between kaons from $\phi$ decays and other kaons, so the $\phi$ meson yields are

TABLE I. Collision species, number of analyzed minimum bias events, accessible $p_T$ range, and typical range of the SB ratio for the different $\phi \to K^+K^-$ analyses.

| Species | $N$ [$10^9$] | $p_T$ [GeV/$c$] | SB | Technique |
|---|---|---|---|---|
| $p + p$ | 1.50 | 0.9–4.5 | 1/9–1/2 | One kaon PID |
| | 1.44 | 1.3–7.0 | 1/76–1/3 | No PID |
| $d$ + Au | 1.69 | 1.1–7.0 | 1/245–1/12 | No PID |
| Cu + Cu | 0.77 | 1.1–2.95 | 1/91–1/9 | One kaon PID |
| | 0.78 | 1.9–7.0 | 1/205–1/24 | No PID |
| Au + Au | 0.72 | 1.1–3.95 | 1/19–1/2 | Two kaons PID |
| | 0.82 | 2.45–7.0 | 1/385–1/32 | No PID |

measured on a statistical basis. In each event, all tracks of opposite charge that pass the selection criteria are paired to form the invariant-mass distribution. This distribution contains both the signal (S) and an inherent combinatorial background (B). To maximize the statistical significance and the reach of the measurements, we use three different track selection techniques: no particle identification (PID) in which all tracks are assigned the kaon mass, but no TOF information is used, and one kaon PID or two kaons PID in which one or both tracks are identified as kaons in the TOF.

Table I lists, for each collision system and for each analysis technique, the number of analyzed minimum bias events in the vertex range $|z_{\rm vtx}| < 30$ cm, the accessible $p_T$ range, and the range of the signal-to-background (SB) ratio.

The raw yields of the $\phi$ are obtained by integrating the invariant-mass distributions in a window of $\pm 9$ MeV/$c^2$ around the $\phi$ mass after subtracting the combinatorial background. In the analysis of Au + Au, Cu + Cu, and $d$ + Au data, the combinatorial background is estimated by using an event-mixing technique. The details of the method are given elsewhere [28]. In the no PID analysis, a significant residual background remains in the subtracted mass spectra because the mixed-event technique does not account for the abundant correlated pairs from other particle decays ($K_s^0 \to \pi^+\pi^-$, $\Lambda \to p\pi^-, \rho \to \pi^+\pi^-, \omega \to \pi^0\pi^+\pi^-$, etc.). In the one kaon PID analysis, the residual background is considerably smaller [38], while in the two kaon PID method, the background is negligible. Examples of subtracted mass spectra obtained in Au + Au collisions with the two kaon PID and no PID techniques are shown in Fig. 1. The SB ratio depends on the collision system, the analysis technique, the $\phi$ transverse momentum, and the centrality. The typical ranges of the SB values for each collision system and each analysis technique are summarized in Table I.

The total combinatorial background in $p + p$ [38] as well as the residual background in $d$ + Au, Cu + Cu, and Au + Au analyses were estimated by fitting the mass spectra with the sum of a Breit-Wigner mass distribution function convolved with a Gaussian experimental mass resolution function to account for the $\phi$ signal and a polynomial function to account for the background. The typical experimental mass resolution for the $\phi$ meson was estimated to be $\sim 1$ MeV/$c^2$ by using Monte Carlo studies based on the known momentum resolution of the tracking system and time resolution of the TOF. To

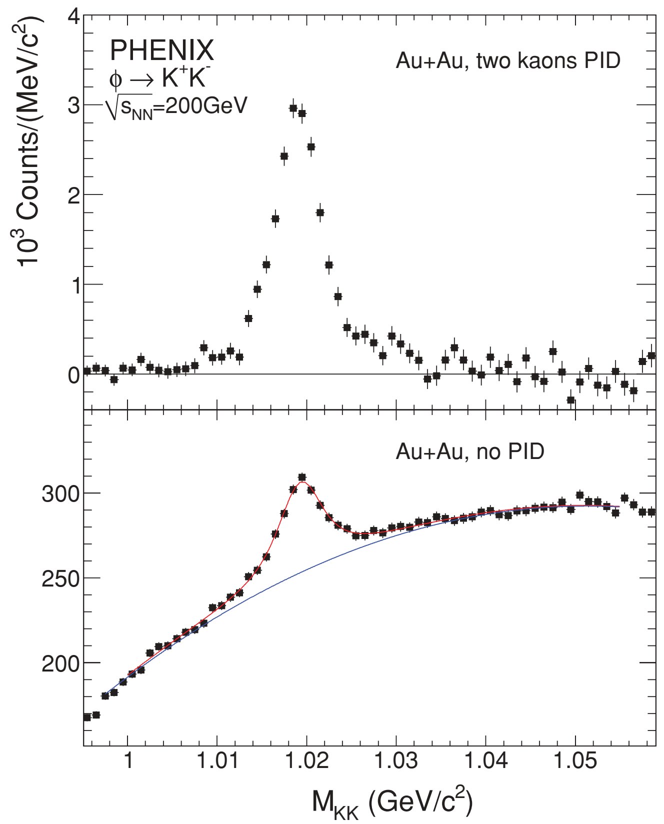


FIG. 1. (Color online) Invariant-mass distributions obtained with the two kaons PID and no PID methods in Au + Au collisions after subtraction of the combinatorial background estimated by using the event-mixing technique. The plot on the top corresponds to integrated $p_T$ range, whereas, the plot on the bottom is for the range $2 < p_T$ (GeV/$c$) $< 3$. The no PID spectrum is fit to the sum of a Breit-Wigner function convolved with a Gaussian function to account for the $\phi$ signal and a polynomial function to account for the residual background.

describe the background, a second-order polynomial was used in most analyses, except for the Au + Au no PID case where a third-order polynomial was used. Figure 1 shows an example of the fits.

The $\phi$ meson invariant yield in a given centrality and $p_T$ bin is obtained by

$$\frac{1}{2\pi p_T}\frac{d^2N}{dp_T\,dy} = \frac{N_\phi C_{\rm bias}}{2\pi p_T N_{\rm evt}\epsilon_{\rm rec}\epsilon_{\rm embed} B_{KK}\,\Delta p_T\,\Delta y}, \quad (1)$$

where $N_{\rm evt}$ is the number of analyzed events in the centrality bin under consideration, $\epsilon_{\rm rec}$ corrects for the limited acceptance of the detector and for the $\phi$ meson reconstruction efficiency, $\epsilon_{\rm embed}$ accounts for the losses in reconstruction efficiency caused by detector occupancy in heavy ion collisions, $B_{KK}$ is the branching ratio for $\phi \to K^+K^-$ in vacuum, $N_\phi$ is the raw $\phi$ yield measured in the given bin, $C_{\rm bias} = \epsilon_{\rm MB}^{\rm BBC}/\epsilon_\phi^{\rm BBC}$, where $\epsilon_{\rm MB}^{\rm BBC}$ and $\epsilon_\phi^{\rm BBC}$ are the BBC-trigger efficiencies for minimum bias and $\phi$ events, respectively. This $C_{\rm bias}$ correction is equal to 0.69 for $p + p$ [39] and varies from 0.92 to 0.85 as we go from peripheral to central $d$ + Au collisions [40]. In Au + Au and Cu + Cu collisions, the minimum bias trigger

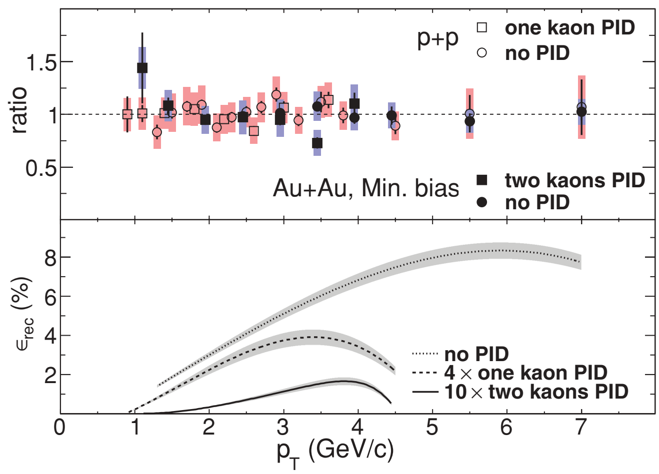


FIG. 2. (Color online) (Top) Ratios of yields obtained with no PID and one kaon PID (in $p + p$ collisions) or no PID and two kaons PID (in Au + Au collisions) to fits to the combined spectra. (Bottom) Comparison of the acceptance and reconstruction efficiencies for the three different analysis techniques.

is inefficient only for very peripheral collisions (centrality $>92.2\%$ for Au + Au and $>94\%$ for Cu + Cu). For all other centralities, 0–92.2% (0–94%) for Au + Au (Cu + Cu), there is no trigger bias, and $C_{\rm bias} = 1$. In $p + p$, the invariant differential cross section at midrapidity is related to invariant yield as $E\,\frac{d^3\sigma}{dp^3} = \sigma_{pp}^{\rm inel} \times \frac{1}{2\pi p_T}\frac{d^2N}{dp_T\,dy}$, where $\sigma_{inel}^{pp} = 42.2$ mb.

The bottom panel of Fig. 2 shows the acceptance and reconstruction efficiencies ($\epsilon_{\rm rec}$) of single $\phi$ mesons, determined by using a full GEANT simulation of the PHENIX detector, which uses different analysis techniques. There are very large differences that reach more than an order of magnitude between the three cases. Despite that, the invariant yield spectra obtained from the different techniques are in good agreement as demonstrated in the top panel of Fig. 2, which shows the ratios of yields obtained with no PID or with one kaon PID (no PID or two kaons PID) techniques in $p + p$ (Au + Au) to a fit performed for the combined data sets. This agreement implies good control over the systematic uncertainties that are quite different in the three cases and provide confidence on the robustness of the experimental results.

The detector occupancy related loss $(1 - \epsilon_{\rm embed})$, which is calculated by embedding simulated $K^+K^-$ pairs into real events, varies from 1% in peripheral to 29% (7%) in the most central Au + Au (Cu + Cu) collisions. No significant $p_T$ dependence of occupancy-induced losses is observed. Consequently, occupancy cannot produce any $p_T$-dependent uncertainties in $R_{\rm AA}$. A similar level of detector occupancy related losses in the number of reconstructed $\phi$ mesons was reported by the STAR experiment [41].

The results from measurements at low $p_T$, which use two kaons PID (in Au + Au collisions) and one kaon PID (in $p + p$ and Cu + Cu) are combined with the independent no PID measurements at intermediate and high $p_T$ to form the final $p_T$ spectra. The measurement in $d$ + Au is performed by using the no PID technique only. The invariant mass spectra obtained with one kaon PID or two kaon PID methods are subsamples of the no PID distribution. Therefore, results obtained with different methods cannot be averaged directly. In the final spectra, the transition between different techniques occurs at $p_T = 1.3$ GeV/$c$ in $p + p$, $p_T = 2.2$ GeV/$c$ in Au + Au, and at $p_T = 3.2$ GeV/$c$ in Cu + Cu collisions to obtain the smallest combined statistical and systematical uncertainties for the points.

Systematic uncertainties on the $\phi$ invariant yield are grouped into three categories: type A (point-to-point uncorrelated), which can move each point independently; type B (point-to-point $p_T$ correlated), which can move points coherently, but not necessarily by the same relative amount; type C (global), which move all points by the same relative amount. The main contribution to the systematic errors of type A is the uncertainty in the raw yield extraction $N_\phi$ of 6%–25%. The error of type B is dominated by uncertainties in reconstruction efficiency $\epsilon_{\rm rec}$ of 5%–9%, embedding corrections $\epsilon_{\rm embed}$ of 1%–7%, and momentum scale of 1%–5%. The main contributions to the type C errors are the uncertainties in normalization for the $p + p$ ($d$ + Au) cross section equal to 9.7% (7.8%) and in branching ratio $B_{KK}$ of 1.2%.

## III. RESULTS AND DISCUSSION

Figure 3 shows the fully corrected $\phi$ invariant yield as a function of $p_T$ measured in $p + p$, $d$ + Au, Cu + Cu, and Au + Au collisions at $\sqrt{s_{_{NN}}} = 200$ GeV. The spectra are scaled by arbitrary factors for clarity and are fitted to exponential and Tsallis [42–44] functions shown by the dashed and solid lines, respectively. We used the Tsallis function adapted to the form [38]

$$\frac{1}{2\pi}\frac{d^2N}{dy\,dp_T} = \frac{1}{2\pi}\frac{dN}{dy}\frac{(n-1)(n-2)}{[nT + m_\phi(n-1)](nT + m_\phi)} \times \left(\frac{nT + m_T}{nT + m_\phi}\right)^{-n}, \quad (2)$$

where $\frac{dN}{dy}$, $n$, and $T$ are free parameters, $m_T = \sqrt{p_T^2 + m_\phi^2}$, and $m_\phi$ is the mass of the $\phi$ meson. The spectral shapes for all collision systems and centralities are well described by the Tsallis function, while the exponential fits underestimate the $\phi$ meson yields at high $p_T$ where the spectra begin to exhibit the power-law behavior expected for particles produced in hard scattering processes. For $p + p$ collisions, the departure from exponential shape occurs at $\approx$4 GeV/$c$. For all centralities in Au + Au collisions, the departure occurs at somewhat larger $p_T$, which suggests a larger contribution of soft processes to the $\phi$ meson production up to 4 to 5 GeV/$c$. Such behavior of the spectral shapes is in agreement with recombination models [22–24,45–47] predicting $p_T$ spectra for different hadronic species based on the number and flavor of their valence quarks. At low transverse momentum, we do not observe a large change in the slopes of the spectra from central to peripheral collisions, supporting the expectation for smaller radial flow of $\phi$ mesons compared to other hadrons.

The large $p_T$ reach of the results presented here allows for the study of medium-induced effects on $\phi$ meson production

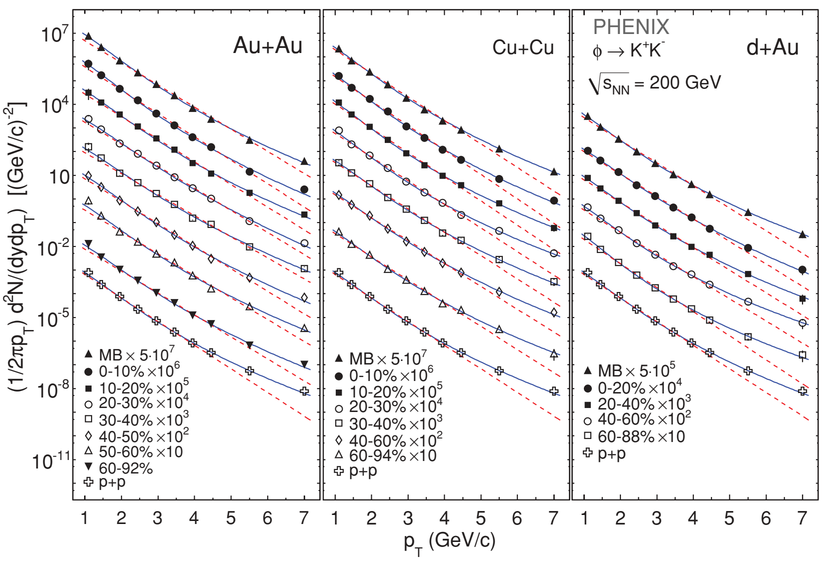


FIG. 3. (Color online) Invariant $p_T$ spectra of the $\phi$ meson for different centrality bins in Au + Au, Cu + Cu, $d$ + Au, and $p + p$ collisions at $\sqrt{s_{NN}} = 200$ GeV. The statistical and systematic uncertainties are smaller than the size of the symbols. The spectra are fitted to exponential and Tsallis [42–44] functions shown by the dashed and solid lines, respectively.

at intermediate and high $p_T$ by using the nuclear modification factor:

$$R_{AB}() = dN_{AB}/(\langle N_{coll}\rangle \times dN_{pp}), \qquad (3)$$

where $dN_{AB}$ $(dN_{pp})$ is the differential $\phi$ yield in nucleus-nucleus $(p + p)$ collisions and $\langle N_{coll}\rangle$ is the average number of nuclear collisions in the centrality bin under consideration [11,12,33]. The latter is determined solely by the density distribution of the nucleons in the nuclei A and B and by the impact parameter and is calculated using the Glauber formalism [48]. Deviation of $R_{AB}$ from unity quantifies the degree of departure of the A + B yields from a superposition of incoherent nucleon-nucleon collisions.

Figure 4 shows a comparison of the $R_{AA}$ for $\phi$ and $\pi^0$ from Ref. [50], proton and kaon from Ref. [33], and $\eta$ from Ref. [51], all measured in Au + Au collisions at $\sqrt{s_{NN}} = 200$ GeV. The $\phi$ meson exhibits a different suppression pattern than that of lighter nonstrange mesons and baryons. For central collisions (top panel), the $\phi$'s $R_{AA}$ shows less suppression than $\pi^0$ and $\eta$ in the intermediate $p_T$ range of $2 < p_T$ (GeV/$c$) $< 5$. At higher $p_T$ values, $p_T > 5$ GeV/$c$, the $\phi$'s $R_{AA}$ approaches and becomes comparable to the $\pi^0$ and $\eta$ $R_{AA}$. These two features remain true for all centralities up to the most peripheral collisions as displayed in the bottom panel of Fig. 4 (see also Fig. 5). The panel shows that the $\pi^0$ is slightly suppressed (at the level of ∼20%) in peripheral Au + Au collisions, whereas, the $\phi$ is not suppressed. The kaon data cover only a very limited range at low $p_T$, but in this range, they seem to follow the $R_{AA}$ trend of the $\phi$ better than that of the $\pi^0$ and $\eta$ for central Au + Au collisions. The comparison with baryons, represented in Fig. 4 by the protons and antiprotons, shows a different pattern. For central collisions, the protons show no suppression but rather an enhancement at $p_T > 1.5$ GeV/$c$, whereas, the $\phi$ mesons are suppressed. This difference between $\phi$ mesons and protons gradually disappears with decreasing centrality, and for the most peripheral collisions, the $R_{AA}$ of $\phi$ and (anti)protons are very similar as demonstrated in the bottom panel.

The results presented here are in agreement with the previous PHENIX results [28], which were based on the

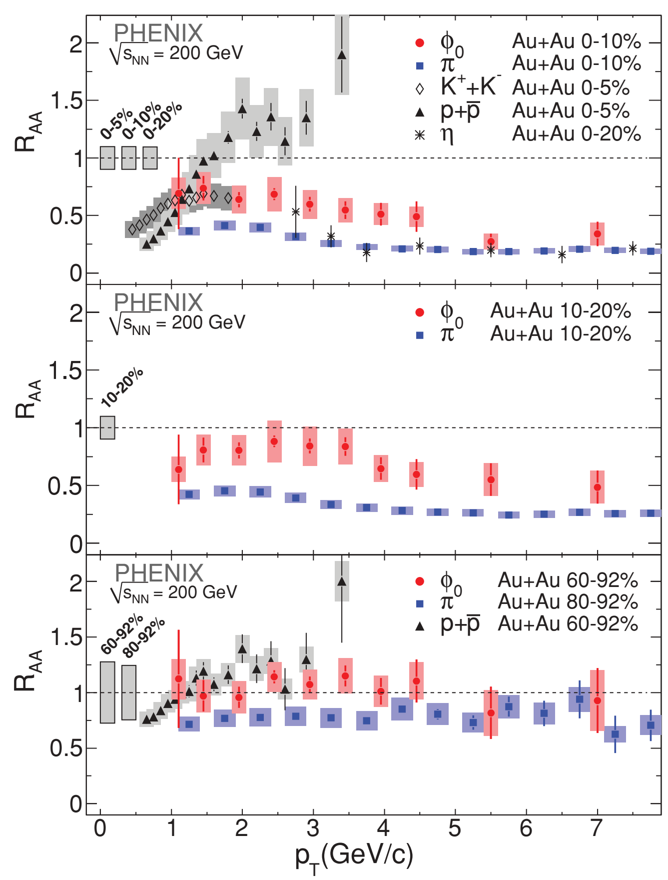


FIG. 4. (Color online) (Top) $R_{AA}$ versus $p_T$ for $\phi$, $\pi^0$, $\eta$, $(K^+ + K^-)$, and $(p + \bar{p})$ in central Au + Au collisions. (Middle) $R_{AA}$ versus $p_T$ for $\phi$ and $\pi^0$ in 10%–20% midcentral Au + Au collisions. (Bottom) $R_{AA}$ versus $p_T$ for $\phi$, and $p + \bar{p}$ in 60%–92% and for $\pi^0$ in 80%–92% peripheral Au + Au collisions. Values for $(K^+ + K^-)$, $(p + \bar{p})$, $\pi^0$, and $\eta$ are from Refs. [12,33,49–51]. The uncertainty in the determination of $\langle N_{coll}\rangle$ is shown as a box on the left. The global uncertainty of ∼10% related to the $p + p$ reference normalization is not shown.

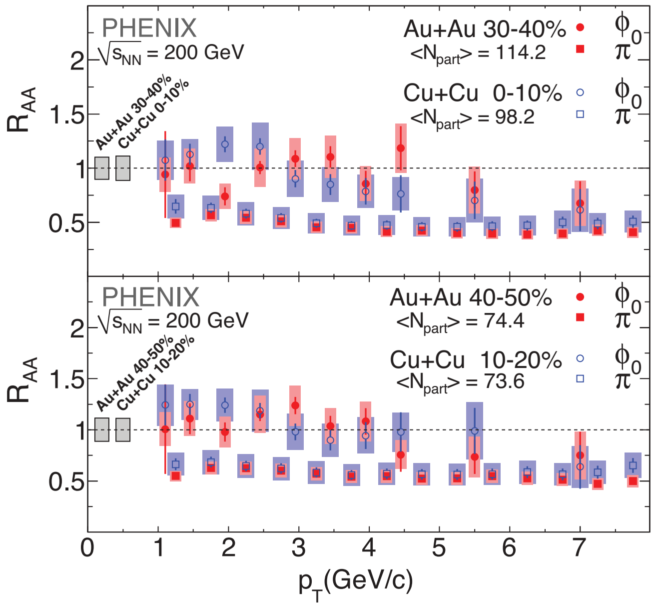


FIG. 5. (Color online) (Top) $R_{AA}$ versus $p_T$ for $\phi$ and $\pi^0$ for 30%–40% centrality Au + Au and 0%–10% centrality Cu + Cu collisions. (Bottom) $R_{AA}$ versus $p_T$ for $\phi$ and $\pi^0$ for 40%–50% centrality Au + Au and 10%–20% centrality Cu + Cu collisions. Values for $\pi^0$ are from Refs. [12,50]. The uncertainty in the determination of $\langle N_{coll}\rangle$ is shown as a box on the left. The global uncertainty of $\sim 10\%$ related to the $p + p$ reference normalization is not shown.

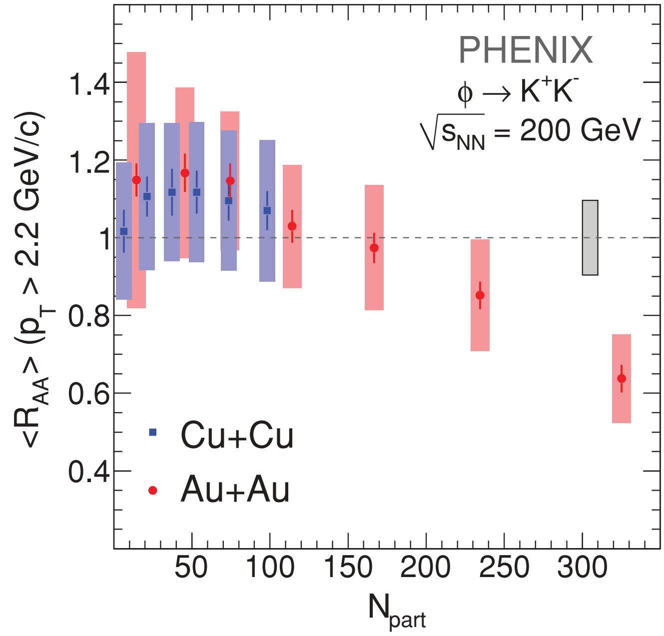


FIG. 6. (Color online) $R_{AA}$ for $\phi$ integrated at $p_T > 2.2$ GeV/$c$ in Cu + Cu and Au + Au collisions versus $N_{part}$. The global uncertainty related to the $p + p$ reference normalization is shown as a box on the right.

2002 RHIC run within the relatively larger uncertainties of the latter. The use of different analysis techniques and the larger Au + Au data sample of the 2004 run resulted in a higher precision and a larger $p_T$ reach of $R_{AA}$ that allowed for unveiling the different behavior of the $\phi$ meson (i.e., less suppression than $\pi^0$ but more suppression than baryons) in the intermediate $p_T$ range. Our results differ from the ones recently published by the STAR Collaboration [29,30], which show that, in Au + Au collisions, $R_{AA}$ is consistent with binary scaling in the intermediate $p_T$ region, whereas, $R_{CP}$ shows considerable suppression. This difference is traced down to the almost factor of 2 higher invariant $p_T$ yield in the STAR experiment [29,30] in Au + Au collisions, compared to our results presented in Fig. 3, whereas, in $p + p$, both experiments are in reasonably good agreement.

Figure 5 compares the $R_{AA}$ of $\phi$ in Au + Au and Cu + Cu in two centrality bins, which approximately correspond to the same number of participants in the two systems. Figure 6 shows the $R_{AA}$ of the $\phi$ integrated for $p_T > 2.2$ GeV/$c$ in Cu + Cu and Au + Au collisions versus $N_{part}$. Under these conditions, there is no difference in the $R_{AA}$ of $\phi$ between the two systems, which indicates that the level of the suppression, when averaged over the azimuthal angle, scales with the average size of the nuclear overlap, regardless of the details of its shape. This behavior has been observed in other measurements, such as the $R_{AA}$ of the $\pi^0$. The $\pi^0$ suppression data in Au + Au and Cu + Cu taken from Refs. [12,50] are also shown in Fig. 5 for comparison. The similarity of the $R_{AA}$ of $\phi$ in the two colliding systems implies that the features discussed previously for Au + Au in the context of Fig. 4, namely, that the $\phi$ exhibits an intermediate suppression between pions and baryons, also remain valid in the Cu + Cu system.

Our data disfavor radial flow as the dominant source for the particle species dependence of the suppression factors at intermediate $p_T$ because the proton and $\phi$ $R_{AA}$ factors differ by a factor of $\sim 2$, despite their similar mass ($m_p \simeq m_\phi$), whereas, the kaon and $\phi$ show similar $R_{AA}$ factors, although their masses differ by almost a factor of 2 ($m_\phi \simeq 2m_K$).

Recombination models [22–24,45–47] qualitatively explain the larger yield of baryons compared to mesons at intermediate $p_T$ by the higher gain in $p_T$ that comes from recombination of three quarks for baryons rather than two quarks for mesons. The same framework can be used to interpret the difference in suppression factors for $\pi^0$ and $\phi$ mesons. For $\pi^0$ production in the Hwa and Yang model [47], the contribution from the recombination of thermal ($\mathcal{T}$) and shower ($\mathcal{S}$) partons becomes comparable to that of the recombination of $\mathcal{TT}$ partons already at $p_T \approx 3$ GeV/$c$. For the $\phi$, however, the strangeness enhancement preferentially feeds the thermal partons. Soft processes dominate over hard processes in a wider $p_T$ range, and consequently, the $\mathcal{TT}$ component remains dominant up to $p_T \approx 6$ GeV/$c$ for the $\phi$ production [46]. The $R_{AA}$ of $\phi$ becomes similar to that for $\pi^0$ at $p_T > 5$ to 6 GeV/$c$ where the contribution from fragmentation partons becomes significant for both particles. It is interesting to note that the $\eta$ closely follows the $\pi^0$ despite its sizable ($\sim 50\%$) strangeness content [52].

Cold nuclear matter effects can also contribute to the differences in hadron suppression factors in A + A collisions. Figure 7 compares the $R_{dA}$ for $\phi$ and $\pi^0$ from Ref. [49] and protons from Ref. [33] for central (top panel) and peripheral (bottom panel) $d$ + Au collisions. For both centralities, the

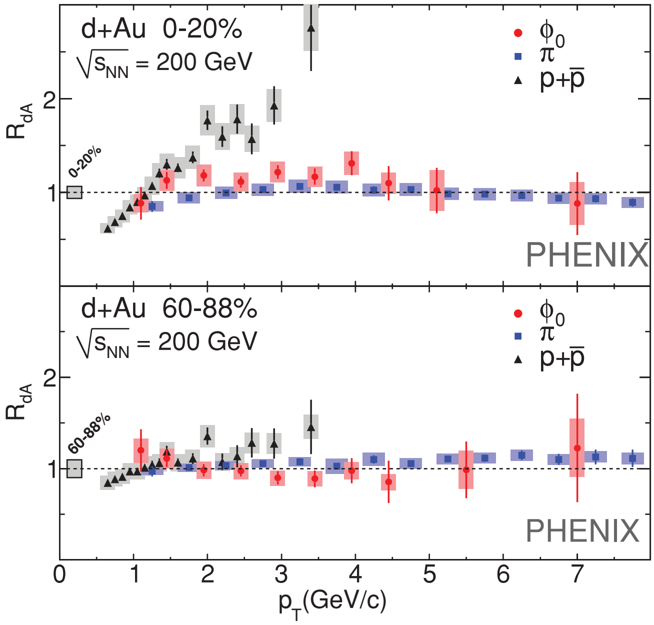


FIG. 7. (Color online) (Top) $R_{\mathrm{dA}}$ versus $p_T$ for $\phi, \pi^0$ and $(p + \bar{p})$ for 0%–20% centrality $d + \mathrm{Au}$ collisions. (Bottom) $R_{\mathrm{dA}}$ versus $p_T$ for $\phi$, $\pi^0$ and $(p + \bar{p})$ for 60%–88% peripheral $d + \mathrm{Au}$ collisions. Values for $(K^+ + K^-)$ and $(p + \bar{p})$ and $\pi^0$ are from Refs. [33,49]. The uncertainty in the determination of $\langle N_{\mathrm{coll}} \rangle$ is shown as a box on the left. The global uncertainty of $\sim$10% related to the $p + p$ reference normalization is not shown.

$R_{\mathrm{dA}}$ for $\phi$ and $\pi^0$ are similar, which indicates that cold nuclear effects are not responsible for the differences between $\phi$ and $\pi^0$ seen in Au + Au and Cu + Cu collisions. The proton's $R_{\mathrm{dA}}$ exhibits an enhancement for $p_T = 2$–$4$ GeV/$c$, usually associated with the Cronin effect [53–58], whereas, the $R_{\mathrm{dA}}$ for $\phi$ indicates little or no enhancement. The lack of Cronin enhancement is also seen in the $\pi^0$ data [49] shown in Fig. 7 and has also been observed for other mesons in central and midcentral $d + \mathrm{Au}$ collisions at $\sqrt{s_{NN}} = 200$ GeV [33,59,60].

## IV. SUMMARY AND CONCLUSIONS

We have measured $\phi$ meson production at midrapidity via the $K^+K^-$ decay channel in $p + p$, $d + \mathrm{Au}$, Cu + Cu, and Au + Au collisions at $\sqrt{s_{NN}} = 200$ GeV. Invariant $p_T$ spectra and nuclear modification factors have been presented over the $p_T$ range of $1 < p_T < 7$ GeV/$c$ for different centralities.

The $\phi$ meson exhibits a different suppression pattern compared to lighter mesons ($\pi^0$ and $\eta$) and baryons (protons and antiprotons) in heavy ion collisions. For all centralities, the $\phi$ meson is less suppressed than $\pi^0$ and $\eta$ in the intermediate $p_T$ range (2–5 GeV/$c$), whereas, at higher $p_T$, $\phi$, $\pi^0$, and $\eta$ show similar suppression values. The available kaon $R_{\mathrm{AA}}$ data seem to follow the $R_{\mathrm{AA}}$ trend of the $\phi$. The comparison with baryons shows that, in central Au + Au collisions, the latter are enhanced with respect to binary scaling, whereas, the $\phi$ meson is suppressed, but this difference gradually disappears with decreasing centrality, and for peripheral collisions, the baryons and the $\phi$ meson have very similar $R_{\mathrm{AA}}$ values consistent with binary scaling.

The same features are observed in Cu + Cu collisions between the $\phi$ and $\pi^0$. The $\phi$ meson invariant $p_T$ spectra in Au + Au and Cu + Cu collisions for similar $N_{\mathrm{part}}$ values exhibit similar shape and yield over the entire $p_T$ range of the measurement within the statistical and systematic uncertainties. This indicates that the production and suppression of the $\phi$ meson, when averaged over the azimuthal angle, scales with the average size of the nuclear overlap region, regardless of the details of its shape.

Cold nuclear effects cannot account for the observed differences. For all centralities, the $\phi$'s $R_{\mathrm{dA}}$ in $d + \mathrm{Au}$ collisions is consistent with binary scaling in agreement with other mesons. No meson species dependence is observed in $R_{\mathrm{dA}}$ within uncertainties.

The observed features at intermediate $p_T$ in Au + Au and Cu + Cu collisions are qualitatively consistent with quark recombination models [22–24,45–47], which are also supported by $\phi$ elliptic flow measurements [29,31]. The systematic set of measurements presented here provides further constraints for these models. The similarity between the suppression patterns of different mesons at high $p_T$ favors the production of these mesons via jet fragmentation outside the hot and dense medium created in the collision. Complementary jet correlation measurements, which involve $\phi$ mesons as a trigger as well as extension of the kaon data to higher $p_T$ would be desirable to provide further insight into the $\phi$ meson production mechanism.

## ACKNOWLEDGMENTS

We thank the staff of the Collider-Accelerator and Physics Departments at Brookhaven National Laboratory and the staff of the other PHENIX participating institutions for their vital contributions. We acknowledge support from the Office of Nuclear Physics in the Office of Science of the Department of Energy, the National Science Foundation, Abilene Christian University Research Council, Research Foundation of SUNY, and Dean of the College of Arts and Sciences, Vanderbilt University (USA), Ministry of Education, Culture, Sports, Science, and Technology and the Japan Society for the Promotion of Science (Japan), Conselho Nacional de Desenvolvimento Científico e Tecnológico and Fundação de Amparo à Pesquisa do Estado de São Paulo (Brazil), Natural Science Foundation of China (People's Republic of China), Ministry of Education, Youth and Sports (Czech Republic), Centre National de la Recherche Scientifique, Commissariat à l'Énergie Atomique, and Institut National de Physique Nucléaire et de Physique des Particules (France), Ministry of Industry, Science and Tekhnologies, Bundesministerium für Bildung und Forschung, Deutscher Akademischer Austausch Dienst, and Alexander von Humboldt Stiftung (Germany), Hungarian National Science Fund, OTKA (Hungary), Department of Atomic Energy and Department of Science and Technology (India), Israel Science Foundation (Israel), National Research Foundation (Korea), Ministry of Education and Science, Russia Academy of Sciences, Federal Agency of Atomic Energy (Russia), VR and the Wallenberg Foundation (Sweden), the US Civilian Research and Development Foundation for the Independent States of the Former Soviet Union, the US-Hungarian Fulbright Foundation for Educational Exchange, and the US-Israel Binational Science Foundation.

---

[1] P. Braun-Munzinger *et al.*, Invited review for *Quark-Gluon Plasma*, edited by R. C. Hwa and X.-N. Wang (World Scientific, Singapore, 2003), Vol. 3, p. 491.
[2] K. Adcox *et al.* (PHENIX Collaboration), Nucl. Phys. A **757**, 184 (2005).
[3] P. F. Kolb and U. W. Heinz, Invited review for *Quark-Gluon Plasma*, edited by R. C. Hwa and X.-N. Wang (World Scientific, Singapore, 2003), Vol. 3, p. 634.
[4] B. Muller and J. L. Nagle, Ann. Rev. Nucl. Part. Sci. **56**, 93 (2006).
[5] P. Huovinen and P. Ruuskanen, Ann. Rev. Nucl. Part. Sci. **56**, 163 (2006).
[6] M. Gyulassy *et al.*, Phys. Lett. B **243**, 432 (1990).
[7] R. Baier *et al.*, Nucl. Phys. B **484**, 265 (1997).
[8] M. Gyulassy *et al.*, Nucl. Phys. B **420**, 583 (1994).
[9] D. d'Enterria (2009), arXiv:0902.2011 [nucl-ex].
[10] K. Adcox *et al.* (PHENIX Collaboration), Phys. Rev. Lett. **88**, 022301 (2001).
[11] S. S. Adler *et al.* (PHENIX Collaboration), Phys. Rev. Lett. **91**, 072301 (2003).
[12] A. Adare *et al.* (PHENIX Collaboration), Phys. Rev. Lett. **101**, 162301 (2008).
[13] S. S. Adler *et al.* (PHENIX Collaboration), Phys. Rev. Lett. **94**, 232301 (2005).
[14] A. Adare *et al.* (PHENIX Collaboration), Phys. Rev. Lett. **98**, 172301 (2007).
[15] S. S. Adler *et al.* (PHENIX Collaboration), Phys. Rev. Lett. **91**, 172301 (2003).
[16] J. Adams *et al.* (STAR Collaboration), Phys. Rev. Lett. **92**, 052302 (2004).
[17] J. Adams *et al.* (STAR Collaboration), Phys. Rev. C **71**, 064902 (2005).
[18] S. S. Adler *et al.* (PHENIX Collaboration), Phys. Rev. C **71**, 051902 (2005).
[19] A. Adare *et al.* (PHENIX Collaboration), Phys. Lett. B **649**, 359 (2007).
[20] T. Hirano and Y. Nara, Phys. Rev. C **69**, 034908 (2004).
[21] U. W. Heinz *et al.*, Nucl. Phys. A **702**, 269 (2002).
[22] V. Greco, C. M. Ko, and P. Levai, Phys. Rev. Lett. **90**, 202302 (2003).
[23] R. C. Hwa and C. B. Yang, Phys. Rev. C **67**, 034902 (2003).
[24] R. J. Fries, B. Muller, C. Nonaka, and S. A. Bass, Phys. Rev. Lett. **90**, 202303 (2003).
[25] I. Vitev and M. Gyulassy, Phys. Rev. C **65**, 041902 (2002).
[26] S. J. Brodsky and A. Sickles, Phys. Lett. B **668**, 111 (2008).
[27] A. Shor, Phys. Rev. Lett. **54**, 1122 (1985).
[28] S. S. Adler *et al.* (PHENIX Collaboration), Phys. Rev. C **72**, 014903 (2005).
[29] B. Abelev *et al.* (STAR Collaboration), Phys. Rev. Lett. **99**, 112301 (2007).
[30] B. Abelev *et al.* (STAR Collaboration), Phys. Lett. B **673**, 183 (2009).
[31] S. Afanasiev *et al.* (PHENIX Collaboration), Phys. Rev. Lett. **99**, 052301 (2007).
[32] C. M. Ko and D. Seibert, Phys. Rev. C **49**, 2198 (1994).
[33] S. S. Adler *et al.* (PHENIX Collaboration), Phys. Rev. C **74**, 024904 (2006).
[34] R. C. Hwa and C. B. Yang, Phys. Rev. Lett. **93**, 082302 (2004).
[35] K. Adcox *et al.* (PHENIX Collaboration), Nucl. Instrum. Methods Phys. Res. A **499**, 469 (2003).
[36] K. Adcox *et al.* (PHENIX Collaboration), Phys. Rev. C **69**, 024904 (2004).
[37] S. S. Adler *et al.* (PHENIX Collaboration), Phys. Rev. Lett. **94**, 082302 (2005).
[38] S. S. Adler *et al.* (PHENIX Collaboration), arXiv:1005.3674 [hep-ex].
[39] S. S. Adler *et al.* (PHENIX Collaboration), Phys. Rev. Lett. **98**, 172302 (2007).
[40] S. S. Adler *et al.* (PHENIX Collaboration), Phys. Rev. Lett. **96**, 012304 (2006).
[41] B. I. Abelev *et al.* (STAR Collaboration), Phys. Rev. C **79**, 064903 (2009).
[42] C. Tsallis, J. Stat. Phys. **52**, 479 (1988).
[43] C. Tsallis, Braz. J. Phys. **29**, 1 (1999).
[44] G. Wilk and Z. Wlodarczyk, Phys. Rev. Lett. **84**, 2770 (2000).
[45] R. J. Fries, B. Muller, C. Nonaka, and S. A. Bass, Phys. Rev. C **68**, 044902 (2003).
[46] R. C. Hwa and C. Yang, arXiv:nucl-th/0602024.
[47] R. C. Hwa and C. B. Yang, Phys. Rev. C **70**, 024905 (2004).
[48] M. L. Miller *et al.*, Ann. Rev. Nucl. Part. Sci. **57**, 205 (2007).
[49] S. S. Adler *et al.* (PHENIX Collaboration), Phys. Rev. Lett. **98**, 172302 (2007).
[50] A. Adare *et al.* (PHENIX Collaboration), Phys. Rev. Lett. **101**, 232301 (2008).
[51] S. S. Adler *et al.* (PHENIX Collaboration), Phys. Rev. Lett. **96**, 202301 (2006).
[52] V. Uvarov, Phys. Lett. B **511**, 136 (2001); arXiv:hep-ph/0105185.
[53] J. W. Cronin *et al.*, Phys. Rev. Lett. **31**, 1426 (1973).
[54] J. W. Cronin *et al.*, Phys. Rev. D **11**, 3105 (1975).
[55] D. Antreasyan, J. W. Cronin, H. J. Frisch, M. J. Shochet, L. Kluberg, P. A. Piroué, and R. L. Sumner, Phys. Rev. D **19**, 764 (1979).
[56] P. B. Straub *et al.*, Phys. Rev. Lett. **68**, 452 (1992).
[57] P. B. Straub *et al.*, Phys. Rev. D **45**, 3030 (1992).
[58] A. Accardi *et al.*, Phys. Lett. B **586**, 244 (2004).
[59] J. Adams *et al.* (STAR Collaboration), Phys. Lett. B **616**, 8 (2005).
[60] J. Adams *et al.* (STAR Collaboration), Phys. Lett. B **637**, 161 (2006).